High-Precision Contour Control by Gaussian Neural Network Controller for Industrial Articulated Robot Arm with Uncertainties

Tao Zhang and Masatoshi Nakamura

Abstract: Uncertainties are the main reasons of deterioration of contour control of industrial articulated robot arm. In this paper, a high-precision contour control method was proposed to overcome some main uncertainties, such as torque saturation, system delay dynamics, interference between robot links, friction, and so on. Firstly, each considered factor of uncertainties was introduced briefly. Then proper realizable objective trajectory generation was presented to avoid torque saturation from objective trajectory. According to the model of industrial articulated robot arm, construction of Gaussian neural network controller with considering system delay dynamic, interference between robot links and friction was explained in detail. Finally, through the experiment and simulation, the effectiveness of proposed method was verified. Furthermore, based on the results, it was shown that the Gaussian neural network controller can be also adapted for the various kinds of frictions and high-speed motion of industrial articulated robot arm.

Keywords: high-precision contour control, gaussian neural network, industrial articulated robot arm, uncertainties

I. Introduction

The contour control is one of the important working patterns for industrial articulated robot arms (IARAs) which have been widely used in industry, such as grinding, cutting, welding, sealing and so on. However, there exist many uncertainties which affect the precision of contour control, especially in the high-speed motion. A main objective of this research is to realize the high-precision contour control by reducing the influence of some uncertainties, such as torque saturation, system delay dynamics, interference between robot links, friction, and so on.

The so-called contour control refers to the movement control of end-effectors which can trace the objective trajectory, along the entirety of operation. The development of contour control is exactly the course of improving the precision and efficiency. Originally, objective trajectories were directly used for the input data without any modification only at low speed operation. With the increasing of speed, the accuracy of the contour control performance becomes low which causes the actual trajectories much distortion as well as low-quality products. In order to solve this problem, many researchers have ever paid more attentions on the proper trajectory generation and made effort to compensate the system delay dynamics[1][2][3]. Despite the fact that there are plenty of trajectory generation algorithms and inverse dynamic control method, these proposed methods are significantly complex, and needing a comprehensive set of link parameters, where some of them are not available in IARAs. Besides, from the experience of view, there also exist many other kinds of uncertainties. For example, interference between robot links and friction can not be neglected when the precision criterion is bigger than a certain threshold or the speed is required to be much higher.

Manuscript received: April 19, 2001., Accepted: Sep. 10, 2001.

T. Zhang and M. Nakamura: Department of Advanced Systems Control Engineering, Graduate School of Science and Engineering, Saga University, Honjomachi, Saga 840-8502, Japan.
(E-mail:zhangtao@cntl.ee.saga-u.ac.jp).

Currently, the called decoupling contour control was proposed in some papers[4][5][6]. The concerned coupling in the decoupling contour control can be called herein as interference between robot links. But in all these methods they are required to identify the model of IARA with interference precisely. Based on such mathematical models, the interference will be compensated by the control signals. Unfortunately, it is hard to obtain so accurate model for the actual operation. There surely exist errors between the model and the actual features of IARA with interference.

Additionally, the influence of friction can not be neglected in view of high precision and high-speed motion of IARA as well. However, modeling of friction is more difficult than that of interference because of not only its nonlinear features but also complex relationship with other factors. At present, many published papers are focus on the friction compensation[7]-[10]. One of effective method is to use observer and real-time feedback control[11]-[13]. But these methods need to attach hardware into the system, such as friction sensors, and there exist velocity limitation for the real-time feedback control. In industry, the technique of servo system has been developed for the real-time control. Generally, the servo system adopted various kinds of feedback control, such as PID control. The friction has been partly compensated in the ordinary conditions. However, with the increase of speed and high demand on the precision, especially for the contour control, the friction compensation by servo system can not be satisfied. With the current level of servo technique, the friction compensation can not be improved further. Therefore, we want to find out other ways to realize the friction compensation for the industrial robot arm with servo system.

At present, integration of artificial neural networks (ANNs) with conventional control design methodologies in the field of robotics has become a notable trend because ANNs have many attractive features, such as ability of learning, approximation of function, robustness, adaptiveness and so on, which are capable

of solving the problems with uncertain factors[14][15]. Therefore, in this research a new contour control method with ANN was proposed to solve the problems of torque saturation, system delay dynamics, interference between robot links, friction and so on in order to make up for all above mentioned shortcomings and improve the practicability in industry. Besides, since we have concentrate on this topic for a long time, in our previous research, system delay dynamics and interference between robot links have been considered by ANN with the ignorance of other uncertainties[16], in current research, we attempt to use ANN controller to overcome various kinds of uncertainties simultaneously and the technique of avoiding torque saturation and compensating friction will be explained and discussed more in detail.

In this research a new contour control method with ANN was proposed to solve the problems of torque saturation, system delay dynamics, interference between robot links, friction and so on in the contour control in order to make up for all above mentioned shortcomings and improve the practicability in industry. Based on this method, various kinds of uncertainties can be overcome simultaneously and high-precision contour control of IARA can be realized in the high-speed motion. Through learning from actual data by ANNs, errors between the model and the actual features of IARA about uncertainties can be reduced, which has been verified by the experiment and simulation results shown in this paper. In addition, the process of the proposed method is not required to change the hardware of IARA because of using off-line feedforward control. The organization of this paper is as below. In section II, the problems of uncertainties were briefly introduced. In section III, the accurate contour control by proper realizable objective trajectory generation, system delay dynamics compensation, interference elimination and friction compensation was explained in detail. In section IV, the effectiveness of proposed method, especially for various frictions, was verified by experiment and simulation. In section V, the features of proposed method were discussed further.

II. Problem statement

1. The reasons of deterioration of contour control performance

For the contour control of IARA, there are two major performances: precision and efficiency. Precision determines the quality of products and efficiency closely relates to the profit. Moreover, the speed of motion is adapted to express the efficiency explicitly. In the industrial applications, working speed of IARA is always required to be high for a higher working efficiency. At high-speed operation, however, the contour control performance of IARA deteriorates because of the influence of some uncertainties. There are many sources of uncertainties, such as torque saturation, system delay dynamics, interference between robot links, external disturbances, friction, gravity, and so on. Because of the utilization of servo system for each link of IARA, the influence of some uncertainties can be reduced[17]. In addition, external disturbances can be also neglected here for simplification. Therefore, in this research the most possible uncertainties in the high-speed operation, such as torque saturation, system delay dynamics, interference between robot links and friction, were considered and our proposed ANN controller has overcome them simultaneously. Besides, two-joint IARA was concentrated to solve these problems in this research.

2. Torque saturation

As we know, the motion of IARA is realized by using servo systems. Servo systems have joint motors, which are actuated with current or voltage controllers that implement torque control of joint motors. The torque which can be performed by joint motor is limited. Therefore, the design of task must consider this pre-defined limitation performance in operation. If the torque is over the maximum of joint motor, the task will be interrupt or torque output of joint motor will keep the maximum. With this situation the actual trajectory was absolutely deteriorated. This phenomenon in industry is always called torque saturation. Torque saturation causes end-effector deviated from the objective trajectory, and consequently brings out tracking deteriorations as well as time lengthening. To maintain accurate contouring, it is necessary that joints should be actuated below their torque/acceleration limits so as to obtain the optimum operation.

3. System delay dynamics

The system delay dynamics refers to the time delay between the control signal and output response. Just because of time delay, the general feedback control can be realized. In some case, system delay can bring out good control performance with feedback output signal. However, in the feedforward control or with the high performance requirement, system delay dynamics will be an unfavorable factor. In order to compensate the system delay dynamics, inverse dynamics control is effective method and its control signal with a certain modification is always called as modified taught signal. At present, the emerged inverse control methods for system delay dynamics compensation were mostly based on the system model. The way of improving the control performance was depended on accurate expression or estimation of system characteristics. In our proposed method, although the basic idea of system delay dynamics compensation was also according to the inverse control, the adopted method was not depended on the improvement of system model but on the learning from actual data generated from actual system. Therefore, even there exists difference between the actual system and system model, the feedforward control can be also realized system delay dynamics compensation with excellent performance.

4. Interference between robot links

The so-called interference considered in this paper refers to the mutually coupling between robot links. The main reasons of interference come partly from the inertial effect and partly from the other forces, such as Coridis and centrifugal force. Through the Euler-Lagrange model of IARA which will be given in section III, interference can be approximated theoretically by many factors, such as the length and mass of link, the position of the center of gravity, joint trajectory, and so on. Comparing with the actual motion of IARA, interference surely can be neglected in the low speed or even in the middle speed without the demand of high precision. However, since the high precision with high speed is just the expected performance in the contour control, interference is an important reason for the deterioration of the contour control performance except for the other uncertainties. Hence, overcoming the interference can improve the contour control performance.

5. Friction

Concerning about friction, there are two things which can cause it in IARA. One is motor and another is load. Gener-

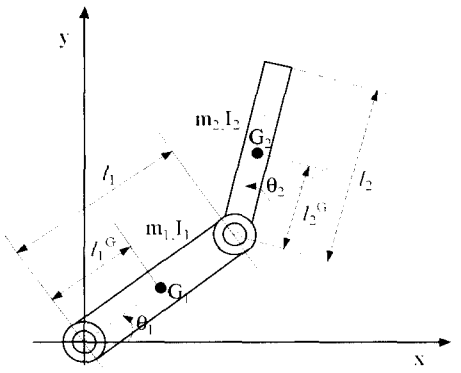

Fig. 1. The two links of industrial articulated robot arm.

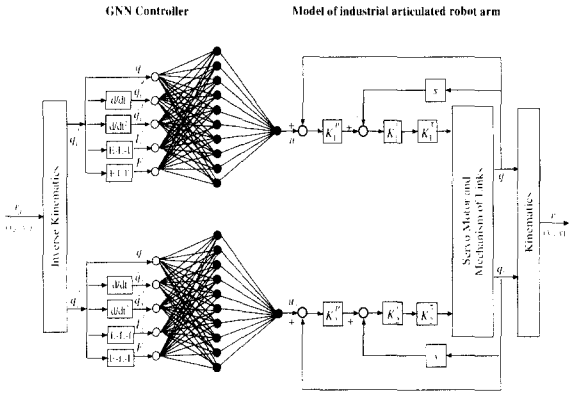

Fig. 2. The model of industrial articulated robot arm and Gaussian neural network controller.

ally, the friction caused by motor is very smaller than the friction caused by load. Therefore, the former friction can be ignored. Besides, owing to existing the well-developed servo system, the influence of friction in actual IARA has been reduced partly. In the low-speed motion, we can neglect it. However, the goal of our research is to fulfill high-precision contour control with the high-speed motion. Therefore, the influence of friction will be surely considered in this paper. Additionally, friction mainly consists of two types: coulomb and viscous. The so-called coulomb friction will be occurred at the moment of transformation of movement pattern. It is related with the velocity transformation direction. The so-called viscous friction will be occurred during the movement. It is highly related with the velocity of movement. In actual system, two kinds of frictions will both affect the movement. Therefore, they were both considered in this research.

6. Realizable objective trajectory generation for torque saturation and Gaussian neural network controller for inverse dynamics, interference and friction

In the contour control of IARA, torque saturation, system delay dynamics, interference and friction mainly affect the performances. Concerning about the torque saturation, proper realizable objective trajectory generation was designed here with the limits of prevailing constraints through the method proposed by [18]. In most realistic applications the constraints contain joint torque limit and assigned velocity. The constraint of joint torque is given by

$$|\tau_j| \leq \tau_{j,max} \tag{1}$$

where τ_j and $\tau_{j,max}$ stand for torque and its limit for j^{th} joint. Torque limit $\tau_{j,max}$ refers to the power amplifier current rating and in the same time the saturation limit of j^{th} joint servo drives. Contouring operations are specified with its assigned velocity v_s. It is required that a contouring operation be bound to its assigned velocity constraint as given by

$$|v_{ec}| \leq v_s \tag{2}$$

where v_{ec} stands for the end-effector velocity. The objective of trajectory generation is to realize accurate contouring performance bound to the constraints (1) and (2).

For the system delay dynamics, interference between robot links and friction, they were considered in the designed controller. In this paper, the Gaussian neural network (GNN) was adopted to control the inverse dynamics of IARA with interference and friction through the feedforward control pattern. The control signal generated by GNN controller not only can compensate the system delay dynamics, but also can eliminate the influence of interference and compensate the friction. The construction of GNN controller and the reasons why it can overcome these uncertainties will be explained in section III.

Additionally, the reason of choosing GNN to construct the controller is mainly concerning the attractive common features of neural network mentioned in introduction and the individual characteristics of GNN[19][20], i.e., well defined activation function and the possibility of systematically selecting the structure and initial parameters. Besides, after learning from actual input/output data of IARA, the GNN controller can successfully achieve the accurate contour control for the system and make up for the errors between the approximated uncertainties by model and actual features.

III. Method

1. Modelling of industrial articulated robot arm

At present, there are many kinds of robot arms which have been used in industry, such as Cartesian coordinate robot, cylindrical coordinate robot, spherical coordinate robot, articulated robot, SCARA robot, and so on. The objective of our research is IARA. Fig.1 shows the IARA with two links. In this figure, l_j, l_j^G, m_j, I_j, θ_j and G_j $(j = 1, 2)$ denote the length of link, the length between the axis and the center of gravity, the mass of link, the inertial moment on the center of gravity, the rotatory angle of link and the center of gravity of link, respectively.

In our research, the model of IARA will be adapted for simulation and defining inverse dynamics of IARA for determination of initial parameters of ANN controller, whose detail explanation will be given later in this paper. Therefore, in this section, we will model the IARA firstly. In our research, the Euler-Lagrange equation[21] is adopted to model the IARA with interference and friction for each link described as (refer to the right side of Fig.2)

$$\begin{cases} [(k_1)^2 J_1^M + m_1(l_1^G)^2 + m_2\{(l_1)^2 + (l_2^G)^2\} + m_1(l_1)^2/3 \\ +m_2(l_2)^2/3]\ddot{q}_1 + K_1^v K_1^\tau \dot{q}_1 + K_1^p K_1^v K_1^\tau q_1 + U_1 \\ = K_1^p K_1^v K_1^\tau u_1 \\ \{(k_2)^2 J_2^M + m_2(l_2^G)^2 + m_2(l_2)^2/3\}\ddot{q}_2 + K_2^v K_2^\tau \dot{q}_2 \\ +K_2^p K_2^v K_2^\tau q_2 + U_2 = K_2^p K_2^v K_2^\tau u_2 \end{cases} \tag{3}$$

where $u_j (j = 1, 2)$ is the control signal, q_j, $\dot{q}_j$, $\ddot{q}_j (j = 1, 2)$

are the actual trajectory, velocity and acceleration, $K_j^p(j = 1,2)$ is the position loop gain, $K_j^v(j = 1,2)$ is the velocity loop gain, $K_j^T(j = 1,2)$ is the torque coefficient, $J_j^M(j = 1,2)$ is the inertial coefficient, $m_j(j = 1,2)$ is the mass of robot link, $k_j(j = 1,2)$ is the gear ratio, $l_j(j = 1,2)$ is the length of robot link, $l_j^G(j = 1,2)$ is the length between the axis and the center of gravity, and $U_j(j = 1,2)$ is the uncertainty of IARA.

And the uncertainty $U_j(j = 1,2)$ contains interference between robot links $I_j(j = 1,2)$ and friction $F_j(j = 1,2)$ which can be described as

$$\begin{cases} U_1 = I_1 + F_1 \\ U_2 = I_2 + F_2 \end{cases} \tag{4}$$

For each link, the interference $I_j(j = 1,2)$ which refers to the coupling in joint coordinate with another joint and friction $U_j(j = 1,2)$ which contains coulomb friction and viscous friction are modeled as

$$\begin{cases} I_1 = (2m_2 l_1 l_2^G \cos q_2)\ddot{q}_1 + \{m_2(l_2^G)^2 + m_2 l_1 l_2^G \cos q_2 \\ \quad + m_2(l_2)^2/3\}\ddot{q}_2 - 2m_2 l_1 l_2^G \dot{q}_1 \dot{q}_2 \sin q_2 \\ \quad - m_2 l_1 l_2^G (\dot{q}_2)^2 \sin q_2 \\ F_1 = D_1 \dot{q}_1 + \mu_1 sgn(\dot{q}_1) \end{cases} \tag{5}$$

$$\begin{cases} I_2 = \{m_2(l_2^G)^2 + m_2 l_1 l_2^G \cos q_2 + m_2(l_2)^2/3\}\ddot{q}_1 \\ \quad + m_2 l_1 l_2^G (\dot{q}_1)^2 \sin q_2 \\ F_2 = D_2 \dot{q}_2 - \mu_2 sgn(\dot{q}_2) \end{cases} \tag{6}$$

where $D_j(j = 1,2)$ is the coefficient of viscous friction and $\mu_j(j = 1,2)$ is the coefficient of coulomb friction.

Besides, kinematics determines Cartesian position and orientation of the end-effectors, given the arm configuration in joint coordinates. It can be described as

$$\begin{cases} x = l_1 \sin q_1 + l_2 \sin(q_1 + q_2) \\ y = l_1 \cos q_1 + l_2 \cos(q_1 + q_2) \end{cases} \tag{7}$$

where l_1, l_2 are the length of robot links, q_1, q_2 are the position of the end-effectors in joint coordinates, and x, y are the position of the end-effectors in Cartesian coordinates.

2. Proper realizable objective trajectory generation

2.1 Trajectory generation for corners

In the contour control, trajectory refers to the movement of end-effectors of IARA. The objective trajectory refers to the desired geometric graph. In order to let end-effectors of IARA realize the movement as objective trajectory, objective trajectory

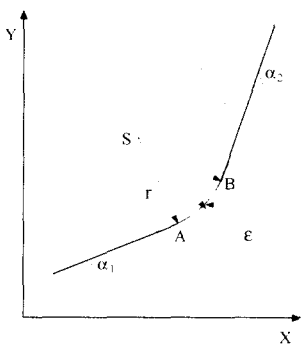

Fig. 3. Trajectory generation for corners by circular path segments with introduced error ϵ.

should be transformed into the realizable objective trajectory. Therefore, the decision process of realizable objective trajectory is called trajectory generation. Generally, trajectory generation at sharp corner always causes torque saturation and performance deteriorations. Therefore, it is proposed that sharp corners are modified by introducing circular path segments as shown in Fig.3.

In Fig.3, the trigonometric relationship between the radius of arc r and introduced error ϵ at the corner is given by

$$r = \epsilon cos\{(\alpha_1 - \alpha_2)/2\}/[1 - cos\{(\alpha_1 - \alpha_2)/2\}] \tag{8}$$

According to the theory of circular motion, the relationship between the maximum Cartesian acceleration of the end-effector $A_{c,max}$ and tangential velocity v_t is as given by

$$A_{c,max} = v_t^2/r \tag{9}$$

In industrial applications there are two categories to determine the tangential velocity v_t and introduced error ϵ at the corner. (1) The maximum Cartesian accelaration $A_{c,max}$ and tangential velocity constraints with a limit $v_{t,min}$ are known. Given $v_t \geq v_{t,min}$, then $r \geq v_{t,min}^2/A_{c,max}$ and $\epsilon = v_{t,min}^2[1-cos\{(\alpha_1 - \alpha_2)/2\}]/[A_{c,max}cos\{(\alpha_1 - \alpha_2)/2\}]$; (2) Given $\epsilon \leq \epsilon_{max}$, where ϵ_{max} denotes a maximum limit for the corner error, then $r \leq \epsilon_{max}cos\{(\alpha_1 - \alpha_2)/2\}/[1 - cos\{(\alpha_1 - \alpha_2)/2\}]$ and $v_t = \sqrt{A_{c,max}r}$. With tangential velocity v_t and radius of arc r , corners can be generated according to uniform circular motion and is given by

$$\begin{cases} x(t) = x(t_1) + rsin\{\alpha_1 + v_t(t - t_1)/r\} - sin\alpha_1 \\ \qquad\qquad (t_1 \leq t < t_2) \\ y(t) = y(t_1) - rcos\alpha_1 - cos\{\alpha_1 + v_t(t - t_1)/r\} \\ \qquad\qquad (t_1 \leq t < t_2) \end{cases} \tag{10}$$

2.2 Trajectory generation for straight-line segments

The trajectory generation for straight-line segments is according to the strategy "maximum joint acceleration strategy" and "assigned Cartesian velocity strategy". Fig.4 shows a straight-line segment P_sP_e. The P_sP_e and P_eP_s are termed as "forward path" and "reverse path" respectively. They are generated in joint coordinate according to "maximum joint acceleration strategy", disregarding assigned velocity constraint. Then, P_1 is located on "forward path" just before (2) is violated. Similarly, P_2 is located on the "reverse path". Then trajectory segment between switching points P_1P_2 is generated in Cartesian coordinate according to "assigned Cartesian velocity strategy". Path segments P_sP_1(start), P_1P_2(middle) and P_2P_e(end) are finally connected together. Besides, the trajectory generation for straight-line segments needs the aid of inverse kinematics and kinematics. Inverse kinematics refers to transformation from the Cartesian coordinate to joint coordinate as

$$\begin{cases} q_1 = \arccos[\{(l_1)^2 - (l_2)^2 + x^2 + y^2\}/\{2l_1\sqrt{x^2 + y^2}\}] \\ \quad + \arctan(x/y) \\ q_2 = \pi - \arccos[\{(l_1)^2 + (l_2)^2 - x^2 - y^2\}/(2l_1 l_2)] \end{cases} \tag{11}$$

The kinematics refers to transformation from the joint coordinate to Cartesian coordinate as equation (7).

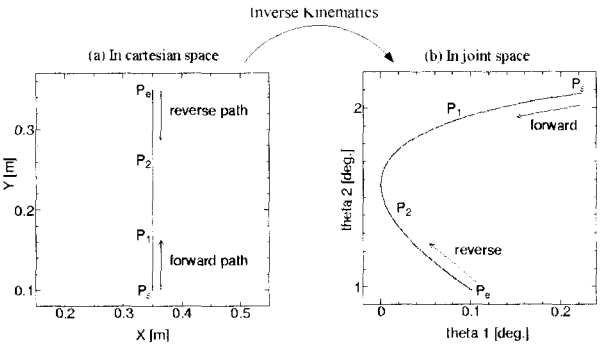

Fig. 4. Trajectory generation for straight line according to the "maximum joint acceleration strategy" and "assigned Cartesian velocity strategy".

In the objective trajectory, the above method was adopted for each sharp corner and each straight line between two sharp corners. Finally, the whole revised trajectory segments are connected for the proper realizable objective trajectory.

3. Construction of Gaussian neural network controller

The Gaussian neural network is a kind of multi-layer feed-forward networks with Gaussian potential function[19]. The network model proposed here is composed of three types of layers: the input layer, the hidden layer, and the output layer. The input and output layers are composed of linear units, and the hidden layer is composed of Gaussian potential function units (GPFUs), which produce Gaussian potential functions. The weighted output values of the GPFUs are summed by the connection between the hidden layer and the output layer in order to synthesize the required potential fields.

The Gaussian neural network controller contains two parts: inverse kinematics and Gaussian neural network (refer to the left side of Fig.2). The inverse kinematics is described as (11). It solves for the arm configuration in joint coordinates, given the position and orientation of the end-effectors in Cartesian coordinates.

The inverse dynamics of the Euler-Lagrange model of IARA is adapted for determination of initial parameters of GNN. If we replace the $[q_j(t)\ \dot{q}_j(t)\ \ddot{q}_j(t)]$ as $[q_j^d(t)\ \dot{q}_j^d(t)\ \ddot{q}_j^d(t)](j=1,2)$ in (3)-(6), where $q_j^d(t)$, $\dot{q}_j^d(t)$ and $\ddot{q}_j^d(t)$ denote the realizable objective trajectory, velocity and acceleration in the joint coordinate respectively, the inverse dynamics of IARA with uncertainties can be obtained as below.

$$\begin{cases} [(k_1)^2 J_1^M + m_1(l_1^G)^2 + m_2\{(l_1)^2 + (l_2^G)^2\} + m_1(l_1)^2/3 \\ +m_2(l_2)^2/3]\ddot{q}_1^d + K_1^v K_1^\tau \dot{q}_1^d + K_1^p K_1^v K_1^\tau q_1^d + U_1^d \\ = K_1^p K_1^v K_1^\tau u_1 \\ \{(k_2)^2 J_2^M + m_2(l_2^G)^2 + m_2(l_2)^2/3\}\ddot{q}_2^d + K_2^v K_2^\tau \dot{q}_2^d \\ +K_2^p K_2^v K_2^\tau q_2^d + U_2^d = K_2^p K_2^v K_2^\tau u_2 \end{cases} \tag{12}$$

And uncertainty $U_j^d(j=1,2)$ in the inverse dynamics of IARA contains interference between robot links $I_j^d(j=1,2)$ and friction $F_j^d(j=1,2)$ which can be described as

$$\begin{cases} U_1^d = I_1^d + F_1^d \\ U_2^d = I_2^d + F_2^d \end{cases} \tag{13}$$

Besides, the approximated interference between robot links $I_j^d(j=1,2)$ and friction $F_j^d(j=1,2)$ in the inverse dynamics of IARA can be described as below.

$$\begin{cases} I_1 = (2m_2 l_1 l_2^G \cos q_2^d)\ddot{q}_1^d + \{m_2(l_2^G)^2 + m_2 l_1 l_2^G \cos q_2^d \\ \quad + m_2(l_2)^2/3\}\ddot{q}_2^d - 2m_2 l_1 l_2^G \dot{q}_1^d \dot{q}_2^d \sin q_2^d \\ \quad - m_2 l_1 l_2^G (\dot{q}_2^d)^2 \sin q_2^d \\ F_1 = D_1 \dot{q}_1^d + \mu_1 sgn(\dot{q}_1^d) \end{cases} \tag{14}$$

$$\begin{cases} I_2 = \{m_2(l_2^G)^2 + m_2 l_1 l_2^G \cos q_2^d + m_2(l_2)^2/3\}\ddot{q}_1^d \\ \quad + m_2 l_1 l_2^G (\dot{q}_1^d)^2 \sin q_2^d \\ F_2 = D_2 \dot{q}_2^d + \mu_2 sgn(\dot{q}_2^d) \end{cases} \tag{15}$$

Although it is capable of getting the inverse dynamics of IARA with interference and friction by the Euler-Lagrange model of IARA, GNN will be adopted to express the inverse dynamics of IARA with interference and friction through the learning from the actual data of IARA instead of them. The following reasons of using GNN are considered. 1) The ideal values of servo system parameters, such as the position loop gain K^p, the velocity loop gain K^v, the torque coefficient K^τ, the friction coefficients D and μ, could not be obtained because of the variance of the manufacturing products; 2) The limitations of position, velocity, acceleration, interference and friction, which are very significant in industry, are not considered; 3) The interference and friction expressed by the Euler-Lagrange model exists error between the model and actual values.

Therefore, the construction of Gaussian neural network contains two steps: determination of initial parameters by the inverse dynamics expressed by the Euler-Lagrange equations of IARA and training. The determination of initial parameters of GNN is based on the method introduced in appendix and the inverse dynamics of IARA expressed by (12)-(15). During the determination of initial parameters of GNN, the structure of GNN can be also defined. In the left side of (12) of the inverse dynamics equations of IARA, there are five items. Each item represents the function of realizable objective trajectory $q_j^d(t)$, velocity $\dot{q}_j^d(t)$, acceleration $\ddot{q}_j^d(t)$, approximated interference $i_j^d(t)$ and friction $f_j^d(t)$, respectively. In order to express the each item by the initial parameters of GNN, the input vector is defined as $\mathbf{x} = [q_j^d(t)\ \dot{q}_j^d(t)\ \ddot{q}_j^d(t)\ i_j^d(t)\ f_j^d(t)]^T$. Therefore, the input of the network for one link is defined with five nodes representing each element of input vector. The coefficient of each element of input vector in the equations of inverse dynamics (12) is defined as a positive constant a and it will be also an important coefficient of initial parameters of GNN. The output of the network has one node representing $u(t)$ which denotes the control signal. With the method of determination of initial parameters explained in appendix, one-input, one-output and two-Gaussian-unit sub-networks are selected for each element of input vector and limitation for each element of input vector will be also considered during the determination of initial parameters of GNN. Therefore, there are five such kinds of sub-networks whose input denote different elements of vector $\mathbf{x}$ and whose output denote part of output of $u(t)$. Then they are combined for expressing the inverse dynamics of IARA with interference and friction. So the hidden layer of GNN has ten Gaussian potential function units.

Besides, in order to learn the true characteristics of IARA with interference between robot links and friction, the actual

sampled output data of IARA for input vector $\mathbf{x}$ and input data for control signal $u(t)$ generated from IARA are adopted as the teaching patterns when we use GNN controller with initial parameters without learning to control IARA for getting sampled data of training. The backpropagation method [16][22] is used for the learning algorithm. Root mean square error is used to measure the progress of learning. The parameters of GNN are updated for each sampled teaching pattern and the algorithm stops when the parameters converge. Through the learning, the GNN realizes the actual inverse dynamics of IARA with interference and friction and provides proper control signals related with objective trajectory to the IARA.

Based on above processes, GNN controller for IARA can be constructed. Such GNN controller has possessed the inverse dynamics of IARA with interference and friction, and can be directly connected with actual system. There are two reasons why GNN controller can overcome some uncertainties. 1) Euler-Lagrange model helps it to obtain the inverse dynamics of IARA; 2) Learning process helps it to reduce the errors between the approximated and actual interference and friction.

4. Utilization of Gaussian neural network controller

After construction of GNN controller, the final control signal $u_j (j = 1, 2)$ generated by GNN controller can overcome uncertainties and be described as below.

$$\begin{cases} u_j(Z_j) = \sum_{i=1}^{10} w_j^i \psi_j^i(Z_j) \quad (j = 1, 2) \\ where: \\ \psi_j^i(Z_j) = exp\{-d_j^i(Z_j)/2\} \\ d_j^i(Z_j) = \sum_{t=1}^{5}\sum_{k=1}^{5} (h_j^i)^{tk}\{x_j^t - (\mu_j^i)^t\}\{x_j^k - (\mu_j^i)^k\}/\{(\sigma_j^i)^t(\sigma_j^i)^k\} \\ Z_j = [x_j^1\ x_j^2\ x_j^3\ x_j^4\ x_j^5]^T = [q_j^d(t)\ \dot{q}_j^d(t)\ \ddot{q}_j^d(t)\ i_j^d(t)\ f_j^d(t)]^T \end{cases} \tag{16}$$

where $Z_j (j = 1, 2)$ denotes the input vector of GNN controller.

Since GNN controller has possessed the inverse dynamics of IARA with interference between robot links and friction and feedforward control pattern is adapted as well, any information from actual system are not required when using GNN controller. As long as the parameters of realizable objective trajectory, such as position, velocity, acceleration, approximated interference and friction, and so on, are not over the limitation defined according to the performance of actual IARA and without torque saturation, then they can be put into the GNN controller. The output of GNN controller u is just the control signal of IARA with interference and friction and the actual trajectory from IARA will be very close to the desired trajectory, i.e., the error between the desired trajectory and actual trajectory is smaller than the performance criterion, which will be verified by the following experiment and simulation.

IV. Results

1. Conditions of experiment and simulation

In order to verify the effectiveness of the proposed method, experiment and simulation has been done by a Performer MK3S IARA produced by Yahata Co., Japan and its Euler-Lagrange model of IARA with interference and friction as (3)-(6). Additionally, since the scale of friction of robot arm in Performer MK3S was too small, the bigger friction than that of ordinary actual robot arm was also assumed for simulation in order to investigate the effectiveness of our proposed method for various kinds of frictions.

The following parameters were given for experiment and simulation: the position loop gains, $K_1^p = K_2^p = 25[1/\mathrm{s}]$; the velocity loop gains, $K_1^v = K_2^v = 150[1/\mathrm{s}]$; the torque constants, $K_1^\tau = 0.104[\mathrm{Nms^2/rad}]$, $K_2^\tau = 0.061[\mathrm{Nms^2/rad}]$; the geer ratios, $k_1 = 160$, $k_2 = 161$; the inertia coefficients, $J_1^M = 4.0 \times 10^{-7}[\mathrm{Nms^2}]$, $J_2^M = 2.7 \times 10^{-7}[\mathrm{Nms^2}]$; the mass of links, $m_1 = 2.86[\mathrm{kg}]$, $m_2 = 2.19[\mathrm{kg}]$; the length of links, $l_1 = 0.25[\mathrm{m}]$, $l_2 = 0.215[\mathrm{m}]$; the length between the axis and the center of gravity, $l_1^G = 0.11[\mathrm{m}]$, $l_2^G = 0.105[\mathrm{m}]$. Therefore, according to (14) and (15), approximated interference I_d and friction F_d can be expressed as

$$\begin{cases} I_1 = 0.115\cos q_2^d \ddot{q}_1^d + \{0.058 + 0.058\cos q_2^d\}\ddot{q}_2^d \\ \quad - 0.115\dot{q}_1^d\dot{q}_2^d \sin q_2^d - 0.058(\dot{q}_2^d)^2 \sin q_2^d \\ F_1 = D_1\dot{q}_1^d + \mu_1 sgn(\dot{q}_1^d) \end{cases} \tag{17}$$

$$\begin{cases} I_2 = \{0.058 + 0.058\cos q_2^d\}\ddot{q}_1^d + 0.058(\dot{q}_1^d)^2 \sin q_2^d \\ F_2 = D_2\dot{q}_2^d + \mu_2 sgn(\dot{q}_2^d) \end{cases} \tag{18}$$

2. Training process

According to the conditions of experiment and simulation, the training trajectory was defined as (see Fig.5)

$$\begin{cases} x_d = R\cos(0.2\pi t) + R\cos(0.2\pi t)/5 \quad (0 \le t \le 10) \\ y_d = R\sin(0.2\pi t) + R\sin(0.2\pi t)/5 \quad (0 \le t \le 10) \end{cases} \tag{19}$$

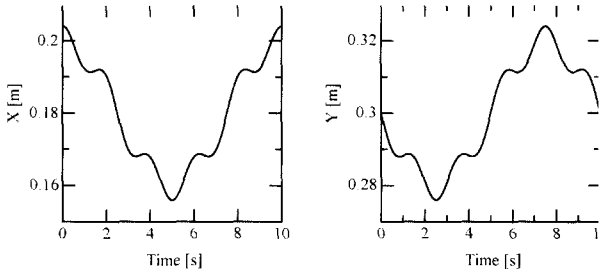

Fig. 5. The training trajectory in the cartesian coordinate.

The radius R of the training trajectory was 2[cm]. After sampling by time interval Δt, the training trajectory and its relative velocity $\dot{q}^d(t)$ and acceleration $\ddot{q}^d(t)$ in joint coordinate calculated by Euler equations as $\dot{q}^d(t) = \{q^d(t) - q^d(t-1)\}/\Delta t$ and $\ddot{q}^d(t) = \{\dot{q}^d(t) - \dot{q}^d(t-1)\}/\Delta t$, and the approximated interference I_d and friction F_d by (14) and (15), were put into the GNN controller with initial parameters. Then the control signals from the GNN controller were put into the actual IARA. Finally, the training patterns consisting of the input/output data of IARA were generated. Besides, the training rate η was selected as a small value of 0.001 because the GNN with the initial parameters closed to the inverse dynamics of IARA [16]. With these training patterns, the parameters of GNN can be updated until convergence. After training process, these parameters of GNN will be fixed for GNN controller.

3. Experiment results

In order to verify the GNN controller, a circle different from the training trajectory was defined as the test trajectory which was described as

$$\begin{cases} x_d = R\cos(0.2\pi t) \quad (0 \le t \le 10) \\ y_d = R\sin(0.2\pi t) \quad (0 \le t \le 10) \end{cases} \tag{20}$$

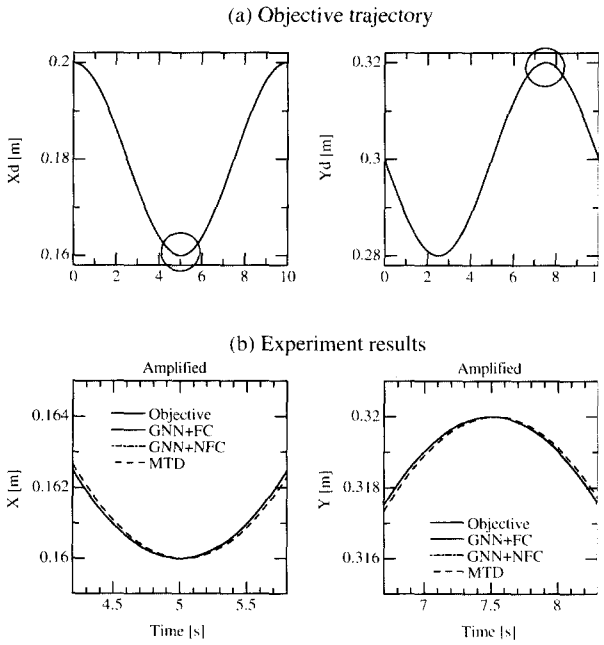

Fig. 6. (a) Objective trajectory (Objective); (b) The experiment results of the GNN controller with friction compensation (GNN+FC), without friction compensation (GNN+NFC) and modified taught data method (MTD) for small friction.

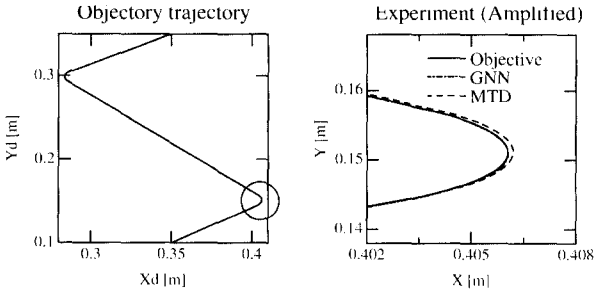

Fig. 7. The objective trajectory (Objective) and experiment results of the GNN controller (GNN) and modified taught data method (MTD) for avoiding torque satuation.

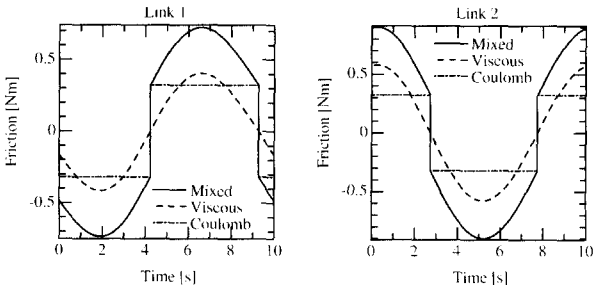

Fig. 8. The approximated mixed friction, viscous friction and coulomb friction.

The radius of the objective circle was also 2[cm]. In the experiment, small friction coefficient with normal speed was considered. The viscous friction coefficients and coulomb friction coefficients were obtained according to actual behavior of IARA beforehand. They were $D_1 = D_2 = 0.008[\mathrm{Nms/rad}]$ and $\mu_1 = \mu_2 = 0.00081[\mathrm{Nm}]$, respectively.

The experiment results were shown in Fig.6. In the figure, there were four kinds of trajectories: objective trajectory (Objective), actual trajectory controlled by GNN with friction compensation (GNN+FC), actual trajectory controlled by GNN without friction compensation (GNN+NFC) and actual trajectory controlled by modified taught data method (MTD) proposed by Goto *et al.* [23]. It is easy to see that the actual trajectory controlled by modified taught data method was deteriorated greatly comparing with objective trajectory. But it is hard to separate other actual trajectories with objective trajectory. Therefore, root mean square error $E^{rms} = \sqrt{\sum_{j=1}^{N} [\{(q_1^d)_j - (q_1)_j\}^2 + \{(q_2^d)_j - (q_2)_j\}^2]/2N}$ was used for calculating the error between the objective trajectory and actual trajectory. The root mean square error between actual trajectory controller by GNN with friction compensation and objective trajectory in experiment was 0.081[mm]. The root mean square error between actual trajectory controller by GNN without friction compensation and objective trajectory in experiment was 0.084[mm]. Therefore, it can be verified that the GNN controller with friction compensation is more effective than the GNN controller without friction compensation. Certainly, it is also more effective than modified taught data method.

Besides, as above mentioned, based on the proper realizable objective trajectory generation, torque saturation can be avoided from objective trajectory in our proposed method. For verifying it, experiment with same parameters as above mentioned was also made, and its friction was omitted because of its small influence comparing with the influence of torque saturation. The objective trajectory with straight lines and corners here was specified by Cartesian points $(0.350[\mathrm{m}], 0.100[\mathrm{m}])$, $(0.410[\mathrm{m}], 0.150[\mathrm{m}])$, $(0.280[\mathrm{m}], 0.300[\mathrm{m}])$ and $(0.350[\mathrm{m}], 0.380[\mathrm{m}])$. The experiment results were shown as Fig.7. From the figure, it is clear that our proposed method is effective to avoid torque saturation and the actual trajectory controlled by our proposed method (GNN) is more accurate than the actual trajectory controlled by modified taught data method (MTD) after the proper realizable objective trajectory generation.

4. Simulation results

In the simulation, big friction coefficient with normal speed was considered. At the same time, not only the influence of friction composed by viscous and coulomb frictions, but also the influence of unique viscous friction and unique coulomb friction were discussed. The viscous friction coefficients were assumed as $D_1 = D_2 = 8.0[\mathrm{Nms/rad}]$ and the coulomb friction coefficients were assumed as $\mu_1 = \mu_2 = 0.8[\mathrm{Nm}]$. In Fig.8 shows the mixed friction, coulomb friction and viscous friction, from which we can know the features of different frictions and it is helpful to understand the influence of frictions on the trajectory. In Fig.9 shows the contour control simulation results of IARA with interference and various kinds of frictions. Fig.9(a) is the simulation results with viscous and coulomb friction. It also contains four kinds of trajectories: objective trajectory (Objective), actual trajectory controlled by GNN with friction compensation (GNN+FC), actual trajectory controlled by GNN without friction compensation (GNN+NFC) and actual trajectory controlled by modified taught data method (MTD) in order to show the effectiveness of our proposed method. Based on the evalu-

Table 1. The comparison of simulation results between the trajectories with GNN friction compensation and without GNN friction compensation for the small friction, big friction and small friction coefficient with high-speed motion.

	Parameters					Evaluation		
	V_{max} [rad/s]	D_1 [Nms/rad]	D_2 [Nms/rad]	μ_1 [Nm]	μ_1 [Nm]	E_{fc}^{rms} [mm]	E_{nfc}^{rms} [mm]	$\frac{E_{nfc}^{rms}}{E_{fc}^{rms}}$
Case 1	0.072	0.0080	0.0080	0.0008	0.0008	0.0211	0.0213	1.010
Case 2	0.072	8.0000	8.0000	0.3200	0.3200	0.0401	0.5540	13.82
Case 3	0.720	0.0080	0.0080	0.0008	0.0008	0.0473	0.1154	2.440

ation of root mean square, the error between actual trajectory controller by GNN with friction compensation and objective trajectory for big mixed friction E_{rms}^{fc} is 0.0401[mm]. The error between actual trajectory controller by GNN without friction compensation and objective trajectory for big mixed friction E_{rms}^{nfc} is 0.5540[mm]. Therefore, our proposed method is quite effect for big friction compensation. Fig.9(b) is the simulation results only with coulomb friction.

Fig.9(c) is the simulation results only with viscous friction. From Fig.9(b) and Fig.9(c) we can see the influence of different frictions clearly. From these figures, it shows the effectiveness of our proposed method and the actual trajectory controlled by our proposed method is almost identical to the objective trajectory.

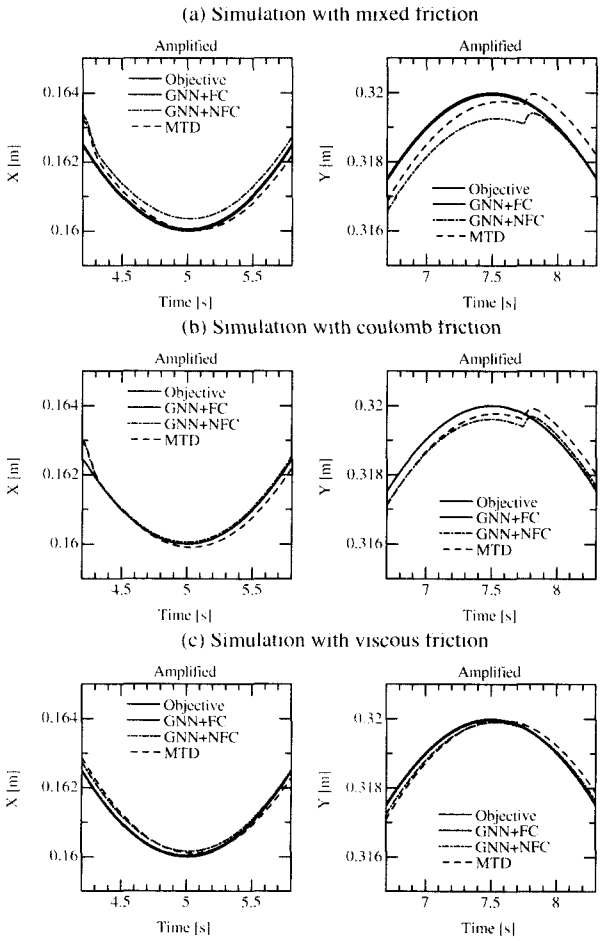

Fig. 9. The simulation results of the GNN controller with friction compensation (GNN+FC), without friction compensation (GNN+NFC) and modified taught data method (MTD) as well as objective trajectory (Objective) for: (a) mixed friction, (b) coulomb friction, (c) viscous friction.

V. Discussion

1. Adaptiveness for small friction coefficient with high-speed motion

High speed is also an important expected performance for the contour control. In above experiment, there was no big difference in the actual trajectories between our proposed method with friction compensation and without friction compensation in the normal speed. But when the speed was increased, the effectiveness of our proposed method with friction compensation became obvious. The friction coefficients were as same as experiment, but the velocity was increased ten times, from 0.072 [rad/s] to 0.72 [rad/s] in joint coordinate. The simulation was shown in Fig.10. From the figure, it was clear to see that the influence of friction was bigger under the high-speed motion and GNN controller with friction compensation (GNN+FC) was more effective than GNN controller without friction compensation (GNN+NFC). Besides, the comparisons of simulation results among the actual trajectory with GNN friction compensation and without GNN friction compensation for the small friction, big friction and small friction coefficient with high-speed motion by root mean square errors were made. The comparison results were shown in Table.1. In the table, we can find the parameters and evaluation results. From the evaluation, the difference between the errors about GNN controller with friction compensation E_{fc}^{rms} and without GNN friction compensation E_{nfc}^{rms} for the small friction, 0.0211[mm] and 0.0213[mm], were not very big, i.e., the times between them $E_{nfc}^{rms}/E_{fc}^{rms}$

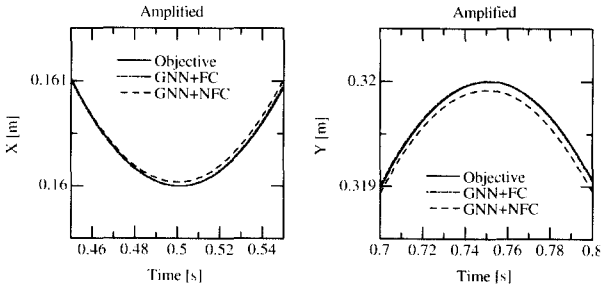

Fig. 10. The simulation results of the GNN controller with friction compensation (GNN+FC) and without friction compensation (GNN+NFC) as well as objective trajectory (Objective) for small friction coefficient with high-speed motion.

was only 1.010. But the difference between the errors about GNN with friction compensation E_{fc}^{rms} and without GNN friction compensation E_{nfc}^{rms} for the big friction, 0.0401[mm] and 0.5540[mm], and for small friction coefficient with high-speed motion, 0.0473[mm] and 0.1154[mm], were quite big. The times between them $E_{nfc}^{rms}/E_{fc}^{rms}$ was also increased, 13.82 and 2.440. From the experiment and simulation results and their comparison, it proves that our proposed method not only can compensate different kinds of frictions, but also can be effective for small friction, big friction and small friction coefficient with high-speed motion of IARA.

2. Advantages and significance of the proposed method

Based on the above explanation and discussion, the advantage and significance of the proposed method for the contour control of IARA are summarized as follows:

- The proposed method can realize the high-precision contour control of IARA with uncertainties, such as torque saturation, system delay dynamics, interference between robot links and friction effectively, which is helpful to improve the quality of product and efficiency.;
- Based on the proper realizable objective trajectory generation, torque saturation can be avoided from objective trajectory;
- Based on the Gaussian neural network controller, system delay dynamics, interference between robot links and friction can be overcome even the model of IARA or the approximated interference between robot links and friction were not accurate;
- The Gaussian neural network controller can also realize the high-precision contour control for IARA with various kinds of frictions and high-speed motion;
- This method is based on the actual data of IARA, which can describes accurately the real features of system and can be easily obtained in industry;
- Since the process of the proposed method is off-line pattern, it is not required to change the hardware of IARA.

VI. Conclusions

A new high-precision contour controller for IARA with uncertainties by using Gaussian neural network has been proposed. With this method, not only torque saturation has been avoided and system delay dynamics has been compensated, but also the influence of interference between robot links has been eliminated and friction has been compensated at the same time. Hence, the precision of contour control was further improved. Owing to learning from the actual sampled input/output data of actual system, the GNN controller can possess the real characteristics of the system. Through experiment and simulation, the effectiveness of the proposed method was verified and some attractive features of the proposed method were also proved. Therefore, the proposed method is very useful for industry.

Appendix

In this appendix, the explanation of how to determine the initial parameters of GNN will be explained. To determine the initial parameters of GNN, one-input, one-output and two-Gaussian-unit sub-networks are selected for each element of input vector $\mathbf{x} = [q_j^d(t)\ \dot{q}_j^d(t)\ \ddot{q}_j^d(t)\ i_j^d(t)\ f_j^d(t)]^T$ (refer to Fig.11). Its input denotes different elements of input vector and its output denote part of output. If define z to represent each element of input vector $\mathbf{x}$, then in each sub-network, the output can be expressed as

$$\begin{cases} f_i(z) = \exp[-(z-\mu_i)^2/\{2(\sigma_i)^2\}] \quad (i=1,2) \\ \phi(z) = w_1 f_1(z) + w_2 f_2(z) \end{cases} \tag{A.1}$$

where w_i, μ_i and $\sigma_i (i = 1, 2)$ denote weight, mean, marginal standard deviation of the ith Gaussian unit of the sub-network, respectively.

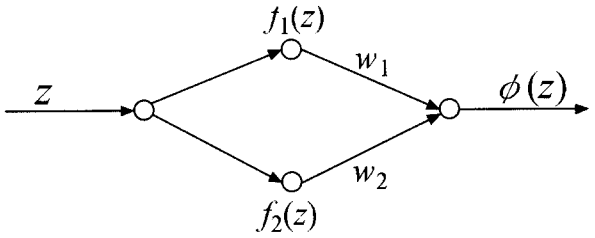

Fig. 11. The sub-network for determination of GNN initial parameters.

In order to express the each item in the equations of inverse dynamics of IARA as (12)-(16) by the initial parameters and add into the limitation for each element of input vector $\mathbf{x}$, the output of each sub-network should be satisfied the condition as $\phi(z) \approx az$ inside of $|z| < Z_{max}$ and $\phi(z)$ converging to zero outside of $|z| < Z_{max}$, where Z_{max} denotes the relative maximum of z and a is a positive constant as the coefficient of a element of input vector $\mathbf{x}$ in the equations of inverse dynamics as (12). Hence, the mean μ_1 is chosen as Z_{max} and μ_2 is chosen as $-Z_{max}$ because the function $\phi(z)$ needs to convergence to zero outside of $|z| < Z_{max}$. The function $\phi(z)$ is approximated as

$$\begin{aligned} \phi(z) \approx & \{w_1 + w_1\mu_1/(\sigma_1)^2\} \exp[-(\mu_1)^2/\{2(\sigma_1)^2\}]z \\ & + \{w_2 + w_2\mu_2/(\sigma_2)^2\} \exp[-(\mu_2)^2/\{2(\sigma_2)^2\}]z \end{aligned} \tag{A.2}$$

by the Taylor expansion of equation (A.1).

Besides, the standard deviation σ_i is selected as $0.57\mu_i$ from the point of view of the sub-network output closing to az and $w_1 = -w_2 = w$ for the unique input in each sub-network[20]. Therefore, comparing with az and based on the following conditions

$$\begin{cases} w_1 = -w_2 = w \\ \mu_1 = -\mu_2 = Z_{max} \\ \sigma_1 = 0.57\mu_1 \\ \sigma_2 = 0.57\mu_2 \end{cases} \tag{A.3}$$

the relationship between the weight of output layer of sub-network and the constant a is obtained as

$$w = (0.57)^2 a Z_{max} \exp[1/\{2 \times (0.57)^2\}]/2 \tag{A.4}$$

Besides, for the input of considered sub-network, the mean μ, standard deviation σ and correlation coefficient h for the Gaussian units in other sub-networks are defined as zero, a large positive constant and zero respectively because there are no any relationship among each sub-network at the initial state.

Acknowledgement

The authors would like to thank Prof. N. Kyura, Department of Electrical Engineering, Kinki University (in Kyushu), Dr. S. Goto, Department of Eletrical and Electronic Engineering, Saga University, and Mr. H. Miyagawa, Yaskawa Electric Co., Japan,

for their constructive comments and Mr. T. Iwanaga, master student of Department of Advanced Systems Control Engineering, Graduate School of Science and Engineering, Saga University, for his help on simulation.

References

[1] D. E. Whitney, "Resolved motion rate control of manipulators and human prostheses," *IEEE Trans. Man Mach. Syst.*, vol. 10, pp. 47-53, June, 1969.

[2] J. Y. S. Luh and C. S. Lin, "Approximate joint trajectories for control of industrial robots along Cartesian paths," *IEEE Trans. Syst.,Man, and Cyber.*, vol. 14, pp. 444-450, June, 1984.

[3] K. G. Shin and N. D. Mckay, "Minimum-time control of robotic manipulators with geomertic path constraints," *IEEE Trans. Automat. Cntr.*, vol. 31, pp. 491-511, June, 1986.

[4] R. Nakashima, M. Ojima, R. Oguro, and T. Tsuji, "A decoupring control method for industrial robots," *T.IEE Japan*, vol. 120-D, no. 5, pp. 673-679, May, 2000 (in Japanese).

[5] S. Goto, M. Nakamura, and M. Obata, "Feedforward compensator for control systems through pole assignment regulator," in *Proceedings of IECON-2000*, pp. 1791-1796, Oct., 2000.

[6] M. Nakamura, M. Obata, S. Goto, and N. Kyura, "Multi-dimensional modified taught data method for mechatronic servo systems: accurate contour control of articulated robot arms by considering interference of links," *T.IEE Japan*, vol. 121-C, no. 1, pp. 90-97, Jan., 2001 (in Japanese).

[7] C. Canudas de Wit, "Adaptive control of partially known system," Boston, USA: Elsevier, 1988.

[8] B. Armstrong, "Control of machines with friction," Boston, USA: Kluwer Academic Publishers, 1991.

[9] M. R. Popovic, K. B. Shimoga, A. A. Goldenberg, "Model based compensation of friction in direct drive robotic arms," *Journal of Studies in Information and Control*, vol. 3, no. 1, pp. 75-88, 1994.

[10] C. Canudas de Wit, H. Olsson, et al, "A new model for control of systems with friction," *IEEE Trans. on Automatic Control*, vol. 40, no. 3, pp. 419-425, 1996.

[11] L. E. Pfeffer, O. Khatib, J. Hake, "Joint torque sensory feedback of a PUMA manipulator," *IEEE Trans. on Robotics and Automation*, vol. 5, no. 4, pp. 418-425, 1989.

[12] D. Vischer, O. Khatib, "Design and development of high-performance torque-controlled joints," *IEEE Trans. on Robotics and Automation*, vol. 11, no. 4, pp. 537-544, 1995.

[13] G. Morel, K. Iagnemma, S. Dubowsky, "The precise control of manipulators with high joint-friction using base force/torque sensing," *Automatica*, vol. 36, pp. 931-941, 2000.

[14] Y. H. Kim and F. L. Lewis, "Neural network output feedback control of robot manipulators," *IEEE Trans. on Robotics and Automation*, vol. 15, pp. 301-309, April, 1999.

[15] M. C. Hwang and X. H. Hu, "A robust position/force learning controller of manipulators via nonlinear H_∞ control and neural networks," *IEEE Trans. on Systems, Man, and Cybernetics*, vol. 30, pp. 310-321, April, 2000.

[16] T. Zhang, M.Nakamura, S. Goto and N. Kyura, "Neural-network controller for articulated robot arm with interference for high-precision contour control," in *Proceedings of the sixth International Symbosium on Artificial Life and Robotics (AROB 6th'01)*, vol. 2, pp. 474-477, Jan., 2001.

[17] J. Z. Zou, M. Nakamura, S. Goto and N. Kyura, "Model construction and servo parameter determination of industrial mechatronic servo systems based on control performance," *Journal of the Japan Society for Precision Engineering*, vol. 64, pp. 1158-1164, Aug., 1998 (in Japanese).

[18] M. Nakamura, R. Munasinghe, S. Goto and N. Kyura, "Feasible method of optimum control of industrial robot arms in operation under speed and torque coonstraints," in *Proceedings of 3rd Asian Control Conference*, pp. 2887-2892, July, 2000.

[19] S. Lee and R. M. Kil, "A gaussian potential function network with hierarchically self-organizing learning," *Neural Networks*, vol. 4, pp. 207-224, Feb., 1991.

[20] S. Goto, M. Nakamura, and N. Kyura, "Accurate contour control of mechatronic servo systems using gaussian networks," *IEEE Trans. On Industrial Electronics*, vol. 43, pp. 469-476, Aug., 1996.

[21] K. S. Fu, R. C. Gonzalez, and C. S. G. Lee, "Robotics: sensing, vision and intelligence," New York: McGraw-Hill Book Co., 1987.

[22] B. Widrow and M. A. Lehr, "30 years of adaptive neural network: perceptron, madaline, and backpropagation," in *Neural Networks*, C. Lau. Ed. New York: IEEE Press, pt.2, pp.27-53, Sept., 1992.

[23] S. Goto, M. Nakamura and N. Kyura, "Modified taught data method for industrial mechatronic servo-controller to achieve accurate contour control performance," in *IEEE/ASME Int. Conf., on Advanced Intelligeng Mechatronics (AIM)*, 525B, June, 1997.

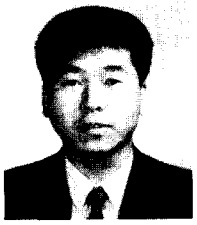

Tao Zhang

He was born in Beijing, China, in 1969. He received B.S., M.S. and Ph.D. degrees in Electrical Engineering from Tsinghua University of China, in 1993, 1995 and 1999, respectively. From 1999, he is pursuing the second Ph.D degree in electrical engineering in the Department of Advanced Systems Control, Graduate School of Science and Engineering, Saga University of Japan. His current research interests include robotics, nonlinear system control theory, neural networks, power system control and maintenance scheduling, and so on.

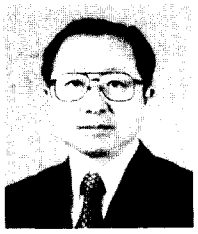

Masatoshi Nakamura

He was born in Fukuoka, Japan, in 1943. He received B.S., M.S. and Ph.D. degrees, all in electrical engineering, from Kyushu University, Fukuoka, Japan, in 1967, 1969 and 1974, respectively. From 1973 to 1974, he was a research associate in Kyushu University. Since 1974, he has been on the Faculty of Saga University, Saga, Japan, and is presently a Professor of Department of Advanced Systems Control Engineering in Graduate School of Science and Engineering in Saga University. His research interests are systems control theory and its applications, especially power system control, thermal flow-control, robotics and biomedical engineering. Prof. Nakamura is a fellow of the Society of Instrument and Control Engineers of Japan, and a senior member of the IEEE Control Systems Society, the Institute of Electrical Engineers of Japan, the Robotics Society of Japan, and the Institute of Systems, Control and Information of Japan.